Article

Kinetics of the Formation and Dissociation of Gas Hydrates from CO$_2$-CH$_4$ Mixtures

Kristine Horvat [1], Prasad Kerkar [1], Keith Jones [1] and Devinder Mahajan [1,2,]*

[1] Materials Science and Engineering Department, Stony Brook University, Stony Brook, New York, NY 11794, USA; E-Mails: khorvat@ic.sunysb.edu (K.H.); kerkarpb@gmail.com (P.K.); jones@bnl.gov (K.J.)

[2] Sustainable Energy Technologies Department, Brookhaven National Laboratory, Upton, New York, NY 11973-5000, USA

* Author to whom correspondence should be addressed; E-Mail: dmahajan@bnl.gov; Tel.: +1-631-632-1813; Fax: +1-631-632-8052.

Abstract: Sequestration of carbon dioxide (CO$_2$) in the form of its hydrates in natural methane (CH$_4$) hydrate reservoirs, via CO$_2$/CH$_4$ exchange, is an attractive pathway that also yields valuable CH$_4$ gas as product. In this paper, we describe a macroscale experiment to form CO$_2$ and CH$_4$-CO$_2$ hydrates, under seafloor-mimic conditions, in a vessel fitted with glass windows that provides visualization of hydrates throughout formation and dissociation processes. Time resolved pressure and temperature data as well as images of hydrates are presented. Quantitative gas conversions with pure CO$_2$, calculated from gas chromatographic measurements yielded values that range from 23 – 59% that correspond to the extent of formed hydrates. In CH$_4$-rich CH$_4$-CO$_2$ mixed gas systems, CH$_4$ hydrates were found to form preferentially.

Keywords: methane hydrate; carbon dioxide hydrate; mixed gas hydrate; carbon sequestration; sodium dodecyl sulfate
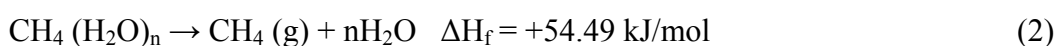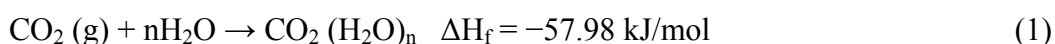
1. Introduction

Much attention has been paid to sequestration of CO$_2$ in saline aquifers, coal beds, and abandoned petroleum reservoirs as a way to curb atmospheric greenhouse effects [1–5]. Specifically, there is

interest in storing CO_2 in gas hydrates on the ocean floor [6] as hydrates can provide a secondary storage method for CO_2 in the ocean, thereby minimizing a chance for stored CO_2 leakage [7].

The chemistry associated with CO_2 hydrate formation is as follows: hydrates are inclusion compounds in which a hydrogen-bonded water cage confines a molecule of CO_2. Hydrate cages are held together by weak van der Waals forces that reduce the free energy of the compound, making it stable at low temperatures and high pressures [8]. Sequestration of CO_2 as a hydrate is, therefore, an attractive method.

Ohgaki *et al*. [9] devised the idea of simultaneously storing CO_2 while extracting CH_4 from deep ocean sediments. The idea is based on the premise that replacing CH_4 gas with CO_2 is a favorable process which will maintain seafloor stability during and after the CH_4/CO_2 exchange, thus minimizing disturbance to the natural environment. Two factors contribute to this hypothesis: (1) structurally, CH_4 and CO_2 gases are similar—both are classified as structure I (sI) hydrate, which consist of two pentagonal dodecahedra (5^{12}) cages and six tetrakaidecahedra ($5^{12}6^2$) cages [8] and (2) hydrates of CO_2 are more thermodynamically stable than CH_4 at temperatures below 10ºC [10]. The phase diagram of CO_2 and CH_4 hydrates in Figure 1 shows the stability zones of both hydrates. As seen in Equations (1) and (2), no additional energy is needed to dissociate CH_4 hydrates, since CO_2 hydrate formation is exothermic and the heat of formation of CO_2 hydrates is enough to dissociate CH_4 hydrates, the latter releases free CH_4 [6]:

$$CO_2 \text{ (g)} + nH_2O \rightarrow CO_2 \text{ (H}_2\text{O)}_n \quad \Delta H_f = -57.98 \text{ kJ/mol} \tag{1}$$

$$CH_4 \text{ (H}_2\text{O)}_n \rightarrow CH_4 \text{ (g)} + nH_2O \quad \Delta H_f = +54.49 \text{ kJ/mol} \tag{2}$$

**Figure 1.** Hydrate stability curves for CO_2 and CH_4 gases.
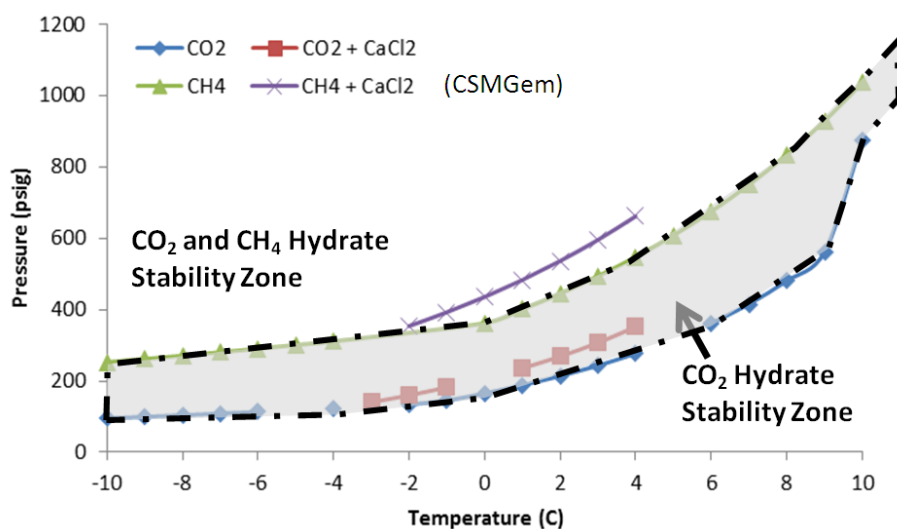
CO_2 molecules prefer the larger $5^{12}6^2$ cages while CH_4 molecules fit easily in the smaller 5^{12} cages. This way, when CO_2 is introduced into the CH_4 hydrate zone, not all of the CH_4 dissociates from its parent hydrate. Lee *et al*. [11] found that nearly 64% of methane gas could be extracted from methane hydrates of composition CH_4 6.05·H_2O. In addition, the reverse reaction, CH_4 gas replacing CO_2 in hydrates, is very slow, so the potential for reformation of CH_4 hydrates is low. CO_2, in general, is thermodynamically a better guest molecule than CH_4 [11].

However, there are many issues that have not been addressed in previous studies. This study focused on the formation of gas hydrates on macroscale, from pure CO_2 and mixed gases (CO_2-CH_4 mixture) in the presence of sodium dodecyl sulfate (SDS), a commonly used hydrate former. Of particular focus was quantitative hydrate formation and decomposition data collection to establish hydrate formation kinetics, P/T stability, and preferential hydrate formation in both pure and mixed gases. Since the pressure vessel in the experimental unit used was fitted with glass windows along the length, time resolved images also complemented this study. Such data would be a useful addition to the CO_2/CH_4 exchange data already known in literature.

2. Materials and Methods

Hydrate experiments on a macroscale were conducted in the Flexible Integrated Study of Hydrates (FISH) unit, shown in Figure 2. The unit was fitted with a series of gas input lines, interchangeable high-pressure cells, and a gas discharge/collection system. The gas input system consisted of CO_2 and CH_4 gas cylinders fitted with a series of valves, pressure regulators, and a flow meter/controller. The conditions inside the Jerguson cell (~198 mL) that served as a high-pressure vessel (Figure 2), could mimic seafloor conditions by confining sediment-water mixture and allowing high-pressure gas (up to 14 MPa) to bubble up the column.

Figure 2. Set-up of the Flexible Integrated Study of Hydrates (FISH) Unit. The heart of the unit is a Jerguson cell fitted with glass windows that served as a high-pressure vessel to mimics seafloor conditions for the runs.
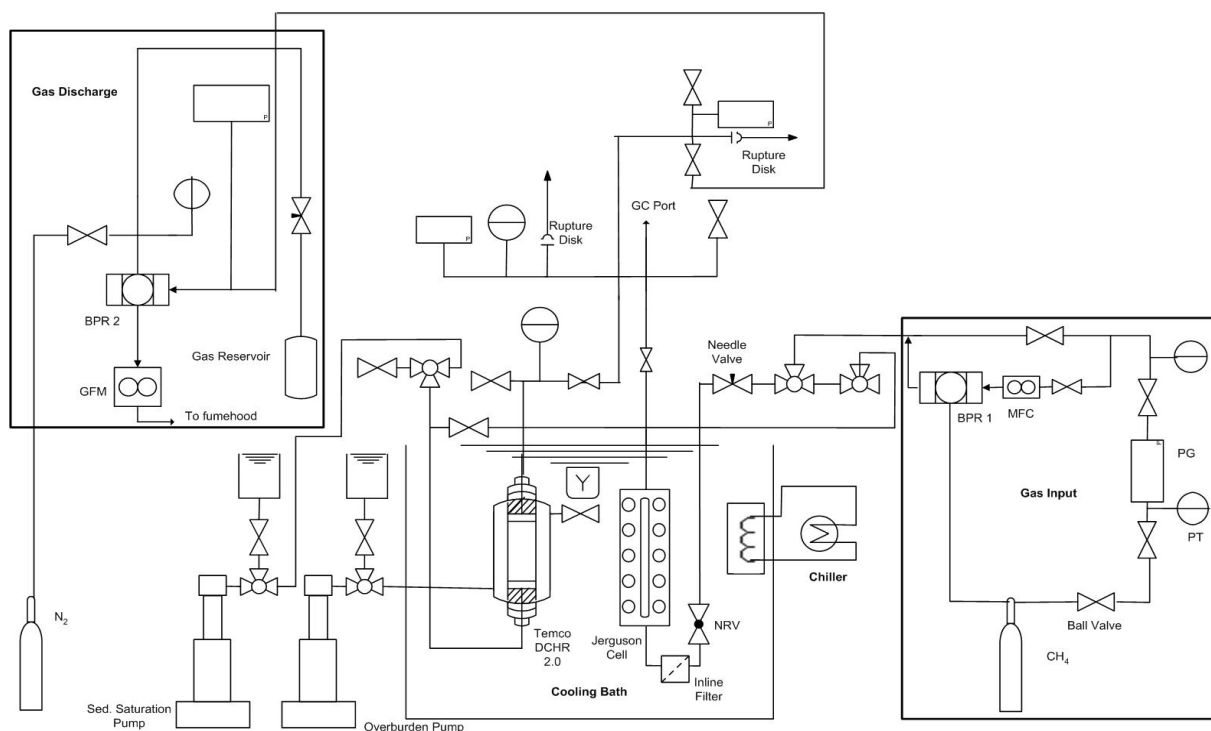
The Jerguson cell was fitted with glass windows along the entire length of the cell that allowed visual monitoring of hydrate formation and decomposition events through acquired images. The pressure transducer at the top of this vessel and several thermocouples located at the top and bottom of

the cell monitored the temperatures of the gas and liquid phases, respectively through a LABView data acquisition system. This cell was kept in a water bath maintained at isothermal temperatures throughout the experiments.

In a typical experiment, a 75 mL aqueous solution of 300 ppm SDS was added into the cell in the unit. Pure gas (CO_2) or gas mixture (CH_4/CO_2) was slowly bubbled into the cell through the solution until a desired operating pressure was attained. The cell was then cooled to attain a temperature between −1 and −2 °C. Hydrate formation continued until the cell pressure asymptoted. At this point, the bath temperature was increased to temperatures above freezing to prevent ice formation. Multiple visual observations were taken throughout the hydrate formation event. In a few runs, the cell was recharged with gas to allow additional hydrate formation. To capture and measure absorbed gas in formed hydrates, the reaction was reversed by dissociation, induced by thermal stimulation of the cell to room temperature.

Gas samples (~0.5 mL) of the free gas from the cell, after formation and during dissociation, were analyzed on a Gow Mac series 580 gas chromatograph (GC) fitted with a Supelco Carbonex 1000 45/60 (1.5 m × 0.32 mm) packed column. The sample analysis procedure involved taking a 0.5 mL gas sample form the headspace of the cell and injecting in the GC. Gas compositions were calculated using pure CH_4 and CO_2 as reference gases.

3. Results and Discussion

A series of hydrate formation runs were performed to study the stability of CO_2 hydrates in a water-SDS solution at ~−1 °C. Table 1 lists experimental Pressure/Temperature (P/T) conditions, theoretical yields, and actual percent conversions achieved.

Table 1. Experimental Conditions and Results from Runs in the FISH unit. (Liquid volume: 75 mL of 300 ppm SDS Solution). * Recharge after Run 1.

Run #	Gas	T_{exp} (°C)	Charge #	Initial Pressure (psig)	Pressure Drop (Δ) (psi)	Measured Conversion (%)	Theoretical Conversion (%)
1	CO_2	−1	1	425	132	30.0	63.6
			2	503	170	32.8	69.0
2	CO_2	−1	*	590	140	23.2	73.5
3	CO_2	−2	1	449	152	32.8	67.9
			2	512	44	8.4	71.7
4	CH_4-CO_2 (62%−38%)	−1	1	992	427	42.4	77.6
5	CH_4-CO_2 (62%−38%)	−1	1	1004	603	59.2	77.9

These high pressure and low temperature conditions resulted in CO_2 hydrates that were observed from gas absorption and visual monitoring through the glass window on the cell. It is thermodynamically clear that gas hydrates formed as the system pressure decreased below the pressure that the system should have remained at for the given temperature conditions.

The volume ratio of gas/water was 1.67 in the cell. The gas/water ratio was maintained to keep experimental conditions in which water, not gas, was in excess. The steps leading to % conversion data are as follows. The first gas charging in Run 1 led to a 30% conversion of CO_2 into hydrates after about 67 h (Figure 3).

Figure 3. P/T *versus* time data plot during gas charging and hydrate formation in Run 1. Cell volume: 198 mL; Water: 75 mL; SDS: 300 ppm; Bath T: +5 °C; Actual cell T: −1 °C; Initial charging P: 425 psig (charge #1); Charge #2: 503 psig.
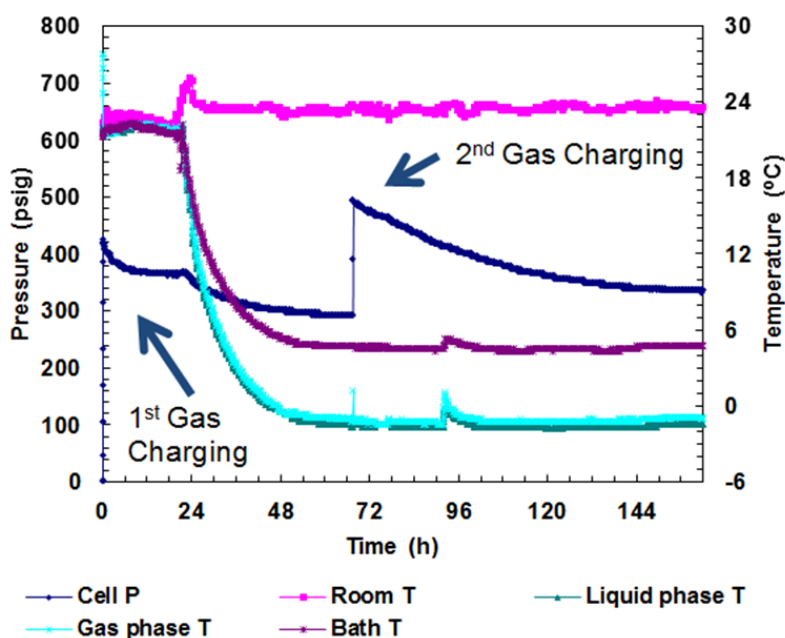

After charging, the initial cell pressure drop from 425 psig to 390 psig was attributed to gas cooling inside the cell. Any further pressure drop under isothermal conditions was attributed to hydrate formation. In the case of Run 1, a total pressure drop of 132 psig was observed over a period of 55 h at −1 °C. After this time period, the cell pressure remained constant over 15 h. At this time after the first charge dropped to below 300 psig, the cell was repressurized to 503 psig at −1 °C. The pressure again dropped, this time to about 344 psig, which remained constant for over 24 h. This second charging resulted in a 33% conversion of CO_2 into hydrates. The cooling was then discontinued and the entire cell was warmed to room temperature. Figure 4 is an image taken after CO_2 hydrates were viewed at the bottom aqueous phase of the cell at around 96 h into the experiment. Figure 5 is a close up of formation cell P/T against time. The images shown in Figure 6 were taken during CO_2 hydrate formation and their thermally induced dissociation. During dissociation, gas bubbles were seen to form uniformly throughout the viewing area in ice pockets as hydrates reverted back to water and CO_2 was released.
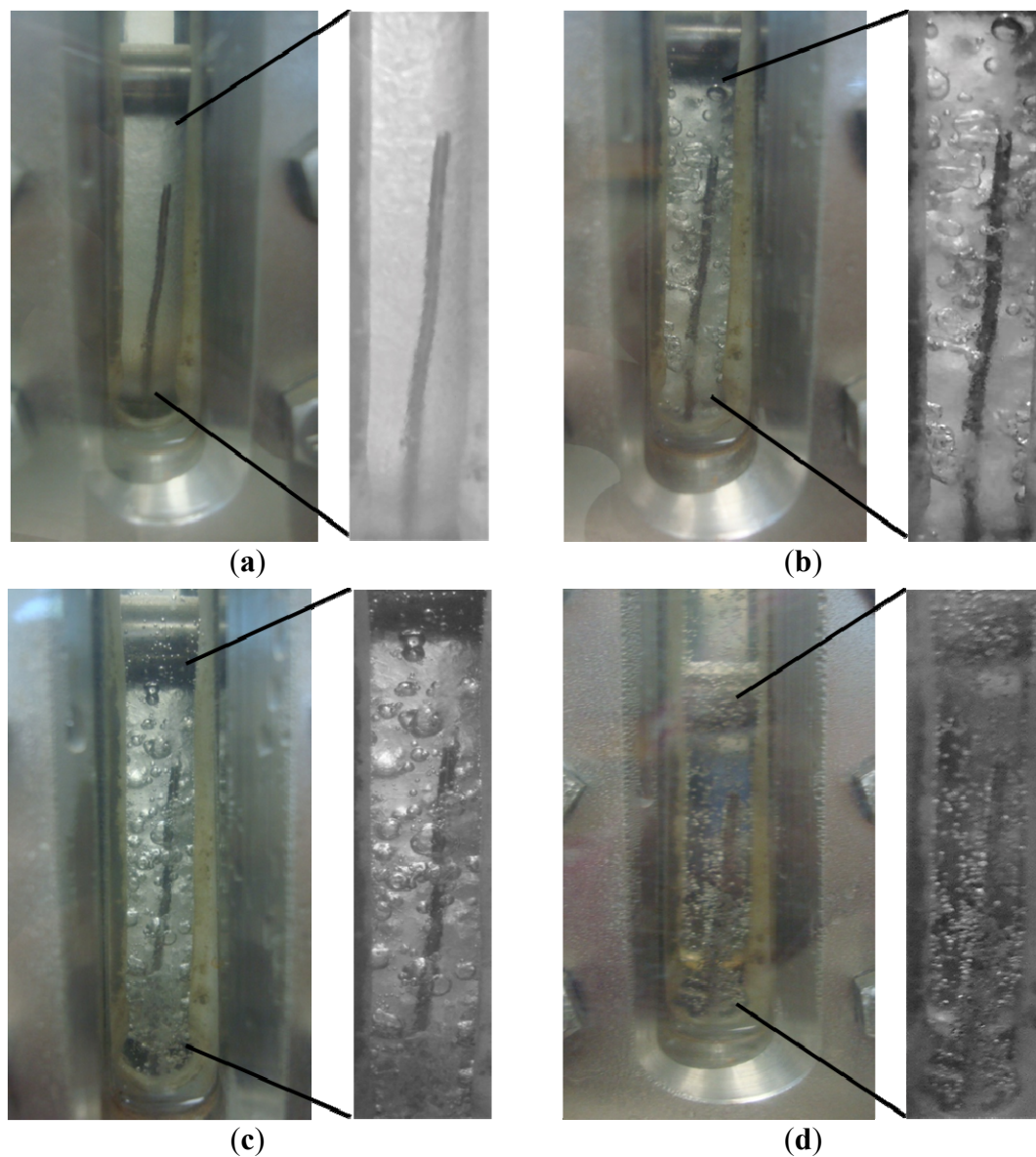
Figure 4. CO_2 Hydrates formed during Run 1. The run conditions are shown in Figure 3. The image on the right is a close up of the hydrates shown in the reactor on the left.
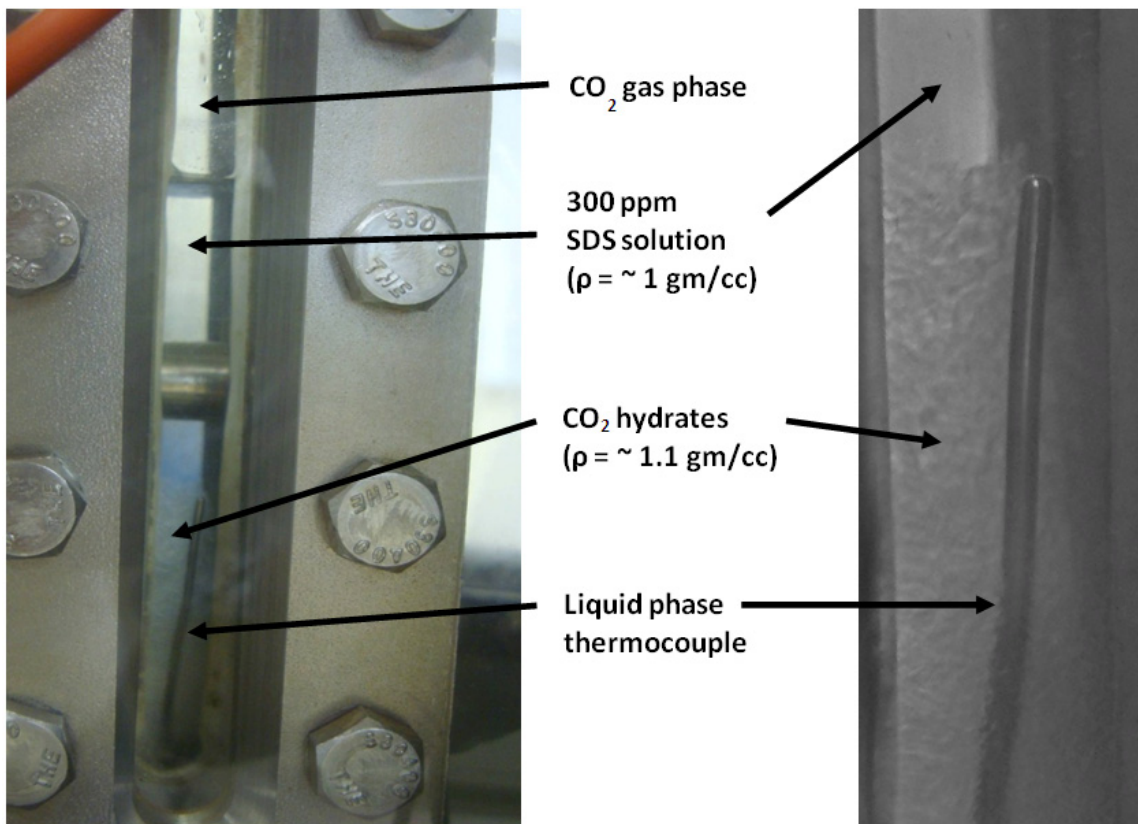
Figure 5. P/T *versus* time data plots during dissociation by thermal stimulation for Run 1. The run conditions are shown in Figure 3.
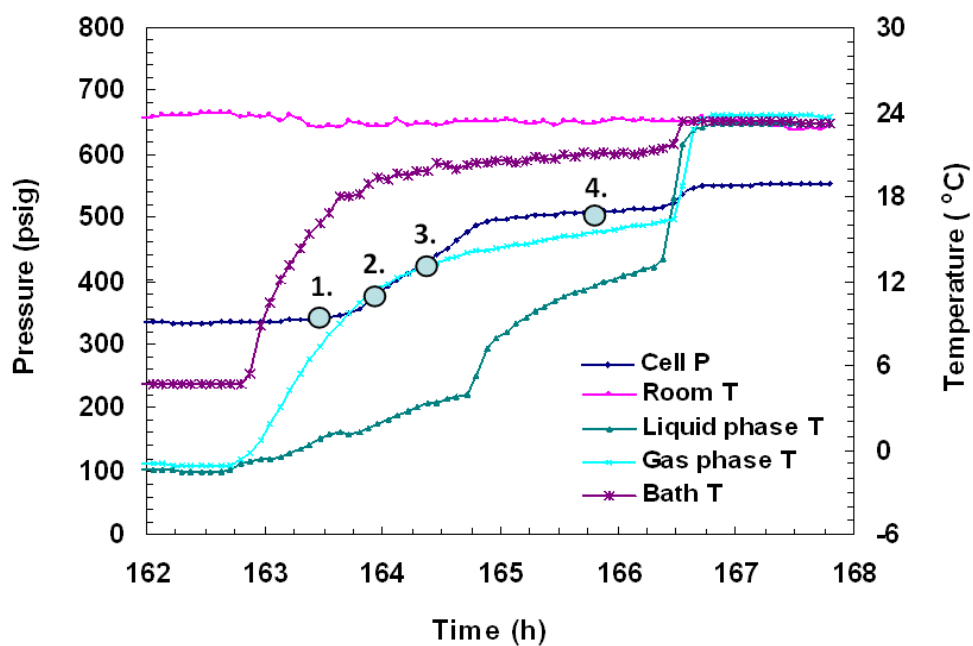
Figure 6. Time resolved visual observations of the CO_2 hydrate phase during Run 1 at (**a**) 339 psig, 5.46 °C; (**b**) 369 psig, 1.62 °C; (**c**) 428 psig, 12.98 °C; (**d**) 508 psig, 15.28 °C. These letters correspond to the numbered P/T conditions shown in the dissociation plot of Figure 5 where point 1 in Figure 5 represents (a) shown below. CO_2 hydrates (density 1.1 g/cc) were observed to have an ice-like appearance in the aqueous phase at temperatures above the freezing point of a water-SDS solution.

(**a**)

(**b**)

(**c**)

(**d**)

Run 2 was performed using the same CO_2 gas and 300 ppm SDS solution that was used in Run 1. Once the cell warmed up to room temperature and all CO_2 hydrates formed during Run 1 had dissociated (no more gas evolution was observed), 40 psi of additional CO_2 gas was added to the system to thoroughly mix the gas/liquid phases inside the cell. Over nine days, the initial cell pressure of 590 psig slowly dropped to 450 psig while the cell temperature was held at −1 °C. At this time, the cell was warmed to increase the temperature to +1 °C (to melt any ice that had formed), leaving only CO_2 hydrates in the cell. A total pressure drop of 140 psig resulted in a hydrate conversion of 23%. Hydrates were observed in the cell, similar to those shown in Figures 4 and 6 for Run 1. Figure 7(a) shows cell the P/T against time data for the entire Run 2.

After the hydrate formation event in Run 2 was complete, the cell was depressurized. The SDS solution used in the previous run was left in the cell and used again in Run 3, and the cell was pressurized to 449 psig with fresh CO_2. After charging, the initial cell pressure drop from 449 psig to 297 psig was attributed to gas cooling inside the cell and hydrate formation. The first gas charging in Run 3 led to a 33% conversion of CO_2 into hydrates as shown in Figure 7(b). A total pressure drop of 152 psig was observed over a period of 42 h at −2 °C. After this time period, the cell pressure remained constant over 30 h. At this time, the cell was repressurized to 512 psig at −2 °C. The initial pressure drop was due to cell cooling but once isothermal conditions were attained, the pressure drop was attributed to hydrate formation. After a total of 144 h, the temperature of the cell was raised to +2 °C to ensure hydrate rather than ice formation. When the temperature was raised above freezing, pressure continued to drop, indicating further hydrate formation until the cell warmed to room temperature. This second charging event only resulted in a hydrate conversion of 8%. Hydrates were visually observed in the cell, similar to those observed during Run1 (Figures 4 and 6).

Figure 7. Cell P/T *versus* Time data plots for: (**a**) Run 2 at −1 °C and 590 psig; (**b**) Run 3 at −2 °C and 512 psig.
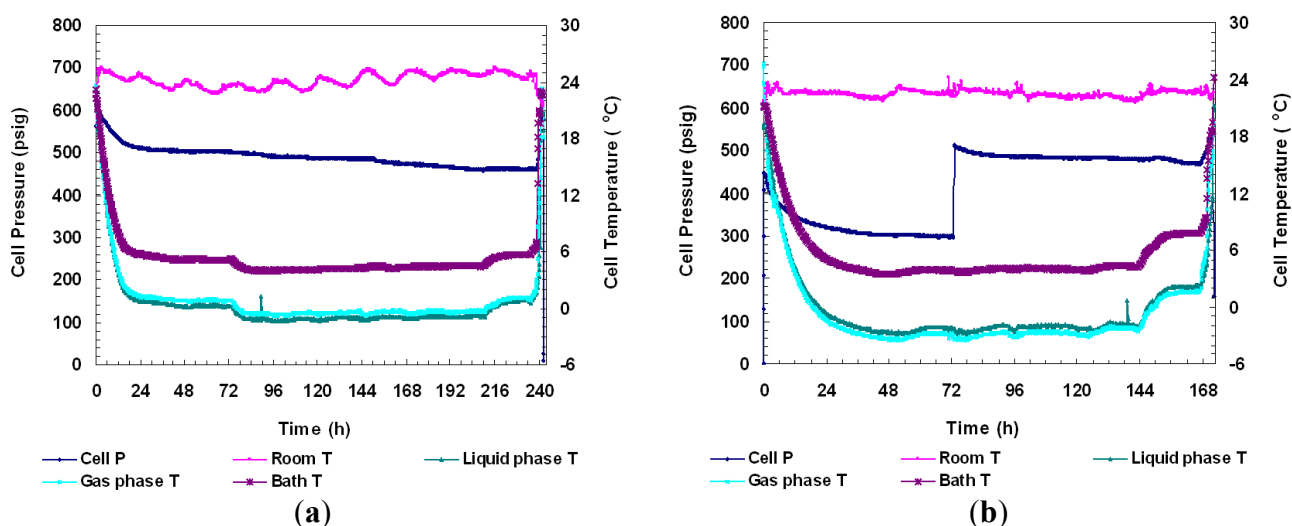
Recharging runs 1 and 3 with CO_2 showed an additional 32% and 8% gas conversion into hydrates respectively. This is expected because these were water-excess systems. Initially, 0.16 to 0.23 moles of CO_2 were charged into the cell while 4.17 moles of solution were present. The ratio for our system of gas to solution is far below the 1/6.05 mole ratio of CO_2 to water needed for full cage occupancy for CO_2 hydrates. The higher charging pressure was found to result in a higher percentage conversion during charge #2 in Run 1 though a low hydrate formation during charge #2 in Run 3 may be due to poor gas-liquid mass transfer. Hydrates are usually found to nucleate at the gas-liquid interface [12], but there is a potential that hydrates nucleated at the gas-liquid interface and then accumulated in the aqueous phase due to density differences between the aqueous phase (1 g/cc) and the CO_2 hydrates (1.1 g/cc). Hydrates have also been hypothesized to nucleate in the aqueous phase by "local structuring" or "labile clustering" [13].

Of the runs with CO_2 (runs 1–3), Run 2 achieved the least conversion (~23%) of CO_2 into hydrates as the solution and CO_2 gas previously used in Run 1 was reused to form hydrates. SDS used as a

promoter in these runs has a tendency to precipitate out of aqueous solutions. This was confirmed in a previous study by Lee *et al*. [14] in which a high concentration of SDS under higher pressures was found to precipitate out earlier than that at lower concentrations. The least conversion observed in Run 2 may be due to the precipitation of SDS after a cumulative 17 days for runs 1 and 2. Also, in this run, SDS precipitation seems to have inhibited the hydrate memory effect. In addition, Wu and Zhang [15] have shown that if the hydrate depleted solution reaches temperatures above 25 °C, the memory effect will not occur. During dissociation, it is possible that the temperature of the cell reached 25 °C.

After successfully forming CO_2 hydrates, runs were conducted to form hydrates from a CH_4-CO_2 mixed gas system. In Run 4, a fresh 300 ppm SDS solution was injected into the cell. The pressure was increased to 380 psig with CO_2 gas, followed by 1000 psig with CH_4 gas, thus forming a mixed gas system. Hydrates were observed in about 2 days after cooling had begun, so the initial cell pressure drop from 992 psig to 810 psig was attributed to gas cooling inside the cell at −1 °C. Any further pressure drop under isothermal conditions was attributed to hydrate formation. Upon initial formation, the cell temperature was increased to +2 °C to thaw the ice phase and confirm hydrate stability and distinguish these from the ice phase. The cell was allowed to equilibrate and pressure remained constant around 750 psig for subsequent 4 days, after which a second drop in pressure was recorded, indicating further hydrate formation. This drop can be clearly seen in the P/T *versus* time plot in Figure 8. After about 3 h of formation, the pressure remained constant for next 24 h at 565 psig, following which the cell was warmed to room temperature. A simple recorded pressure difference and change in the number of moles of gas present in the cell at the end of formation were calculated to show that 42% of the initial gas converted into hydrates, though CO_2 and CH_4 were indistinguishable.

Figure 8. A plot of P/T *versus* time during charging and hydrate formation in Run 4. Hydrate formation was achieved from a CH_4-CO_2 mixture. The embedded pink dots represent gas compositions measured by analyzing gas samples at corresponding times.
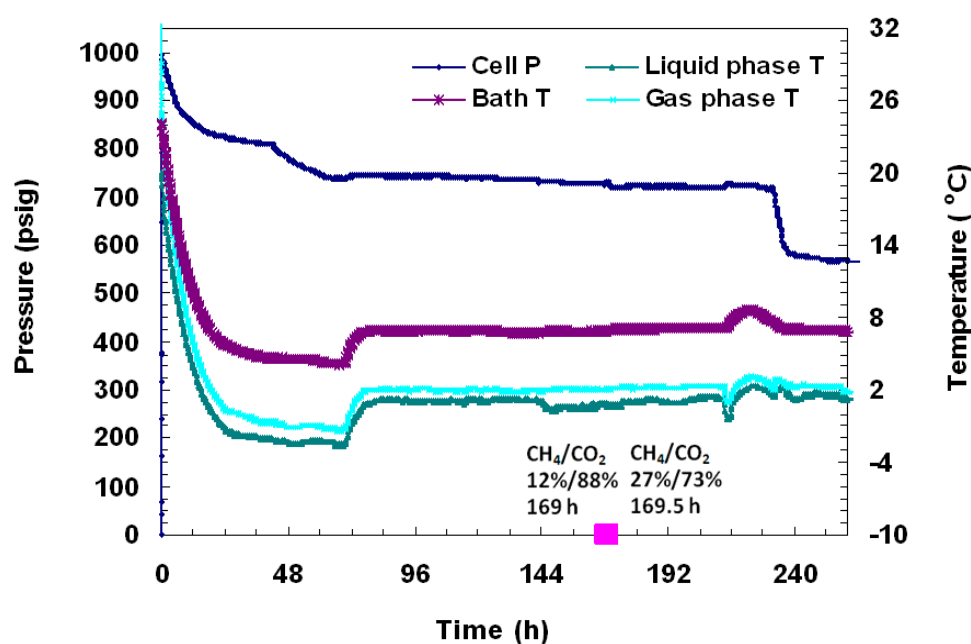
To discern the identity of hydrates, several gas samples (0.5 mL) were taken from the vessel and analyzed during formation and dissociation. The gas chromatographic (GC) data as %volume change from initial and final gas values for each gas are shown in Figures 8 and 9. In Figure 8, it was found that at 169 h into the experiment when cell pressure was 748 psig and cell temperature was +1 °C, the gas phase of the cell consisted of 12% CH_4 and 88% CO_2. Subsequently, 30 minutes later, under the same P/T conditions, another gas sample was taken and was found to be made up of 27% CH_4 and 73% CO_2. This indicates that initially, CH_4 hydrates form, but as formation continues in the cell, more CO_2 gas replaces CH_4 in hydrates. Following the second pressure drop, three more GC gas samples were taken in Figure 9. The first gas sample, taken 284.5 h into the experiment at 568 psig and +1.4 °C, showed the gas composition as 66% CH_4/34% CO_2. One hour later, a sample taken at 567 psig and +1.3 °C showed the gas composition as 63% CH_4/37% CO_2. The last gas sample, taken 1.5 h after thermal stimulation had begun at 638 psig and +1 °C, showed gas as 68% CH_4/32% CO_2. Similar concentrations of CH_4 and CO_2 before and after formation were measured with GC analysis, which confirm similar relative % conversions for both gases. Embedded in Figure 10 are images taken of the gas hydrates that formed in the vessel over time. The numbered points in Figure 9 represent the conditions for the lettered images in Figure 10 where point 1 in Figure 9 corresponds to image (a) of Figure 10.

Figure 9. P/T against time during dissociation by thermal stimulation in Run 4. Hydrate formation was achieved from a CH_4-CO_2 mixture. The embedded pink dots represent gas compositions measured from gas samples analyzed in a Gow-Mac 580 series gas chromatograph.
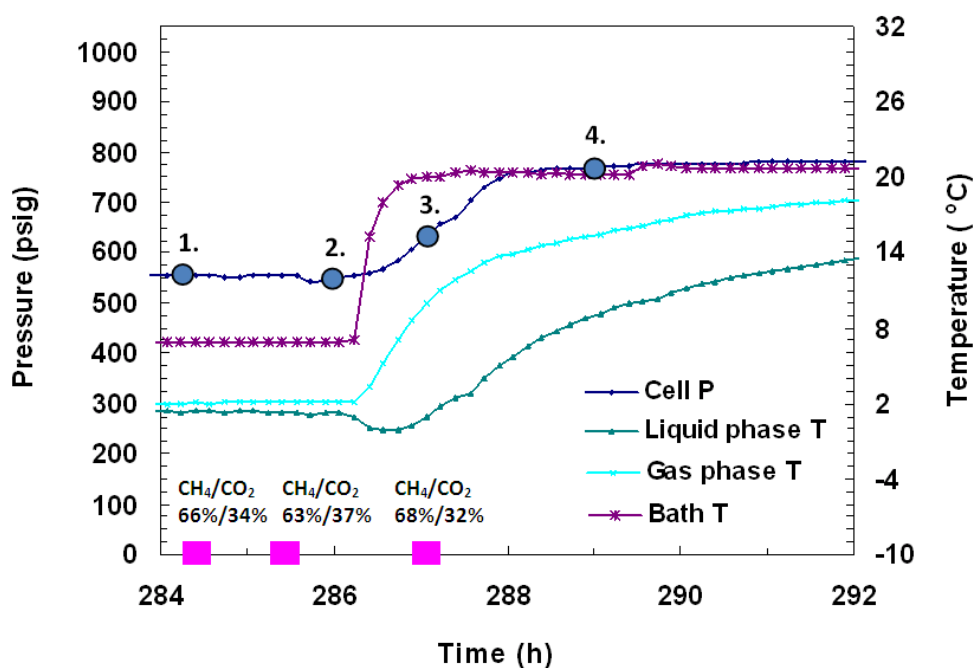
Figure 10. Time-resolved observations of the CH$_4$-CO$_2$ hydrate formation at the end of formation and during dissociation in Run 4 at (**a**) 574 psig, 1.38 °C; (**b**) 559 psig, 1.34 °C; (**c**) 629 psig, 0.77 °C; (**d**) 770 psig, 8.92 °C. These P/T conditions correspond to the numbers shown in the dissociation plot of Figure 9 where point 1 in Figure 9 represents (a) shown below.

(**a**)

(**b**)

(**c**)

(**d**)
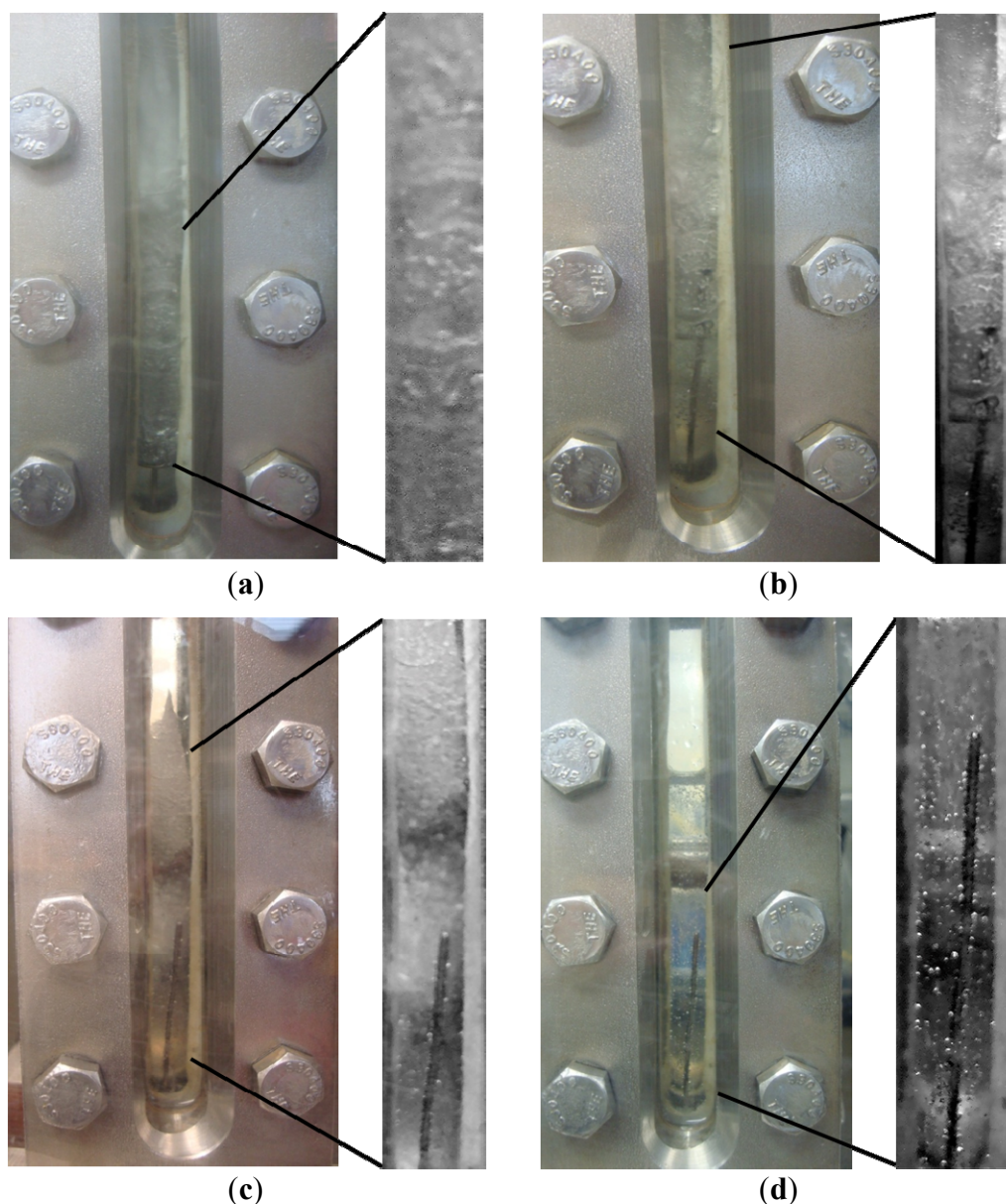
Run 5 was performed using the same procedure as described for Run 4. In this case, the cell was pressurized to 380 psig with CO$_2$ gas, followed by 1000 psig CH$_4$ gas. Hydrates formed a day after cell cooling began. As shown in Figure 11, a pressure drop from 1004 psig to 880 psig due to cooling to −1 °C was observed over the first 24 h, followed by an abrupt pressure drop to 475 psig which was attributed to hydrate formation. A pressure of 410 psig was maintained for two days, after which the cell temperature was increased to +2 °C to confirm the presence of the hydrate phase. Once the cell was warmed above freezing, pressure remained stable at 565 psig for 24 h until the run ended. An overall gas conversion of 59% into hydrates was achieved.

Figure 11. (**a**) A plot of P/T *versus* time during charging, formation, and dissociation from a CH_4-CO_2 mixture in Run 5; (**b**) A close-up view of hydrate dissociation by thermal stimulation. The embedded pink dots represent calculated gas compositions from gas chromatographic data.


(**a**)

(**b**)
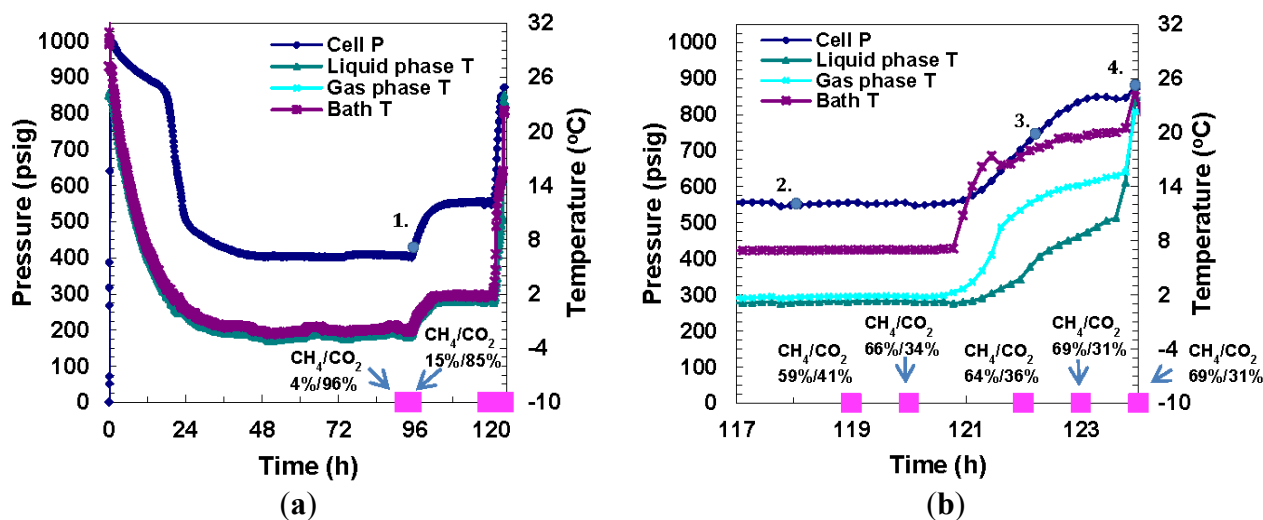
As described for the previous run, several gas samples were analyzed during formation and dissociation to calculate individual % gas (CO_2 or CH_4) that converted to hydrates. Figure 11 shows P/T *versus* time plots and Figure 12 shows images of gas hydrate formation over time for Run 5, a mixed gas system. In Figure 11a, a gas sample was taken 94 h after the experiment had begun at 417 psig and −2.5 °C and the gas composition was measured to be 4% CH_4/96% CO_2. Two hours later, at 406 psig and −2.7 °C, the gas composition was 15% CH_4/85% CO_2. Similarly in Run 4, CH_4 hydrates were seen to form in the earlier stages of formation, and as time went by, more CO_2 hydrates formed. At this point, the cell temperature was raised to above freezing to ensure that the ice phase was not present in the cell. Five GC samples were taken prior to and during dissociation as shown in Figure 11b, which is a close up of day five of the experiment. The gas compositions under P: 566 psig and T: +1.3 °C, at various time intervals were as follows: (1) Sample #1, Time: 119 h: 59% CH_4/41% CO_2; (2) Sample #2: Time: 120 h: 66% CH_4/34% CO_2. At this point, thermal stimulation was begun to bring about dissociation of formed hydrates. At 122 h, the temperature was 2.4 °C, the pressure increased to 644 psig and the gas analysis was: 64% CH_4/36% CO_2. At 123 h, the pressure was 811 psig at +7.7 °C and the corresponding gas analysis was: 69% CH_4/31% CO_2. At 124 h, the pressure had increased to 860 psig as the temperature increased to +10.2 °C but the gas analysis was unchanged. The numbered points in Figure 11a and 11b represent P/T conditions in the cell when the lettered images in Figure 12 were taken where point 1 in Figure 11 corresponds to image (a) of Figure 12.

The hydrate formation runs with 62% CH_4/38% CO_2 gas mixtures resulted in gas conversions as high as 42% and 59%. Hydrates from the CH_4-CO_2 mixture were found to grow uniformly throughout the cell as a massive structure. A solid structure in the form of hydrates was visually observed on the entire the viewing glass (1/2 in. × 12 in.). Dissociation was also observed randomly throughout the hydrate phase. Both CO_2 hydrates and CH_4 hydrates were indistinguishable in terms of morphology to the naked eye, so it is unknown if CO_2 and CH_4 hydrates or mixed gas hydrates formed.

It is apparent from the completed runs in the FISH unit that facile formation of both CO_2 and CH_4 hydrates was observed, under the P/T conditions used. It was found that, especially in the early stages of hydrate formation, a majority of the gas that was stored in hydrates was CH_4. Seo *et al.* (2001) [16] observed that at lower pressures, CO_2 preferentially forms hydrates. Uchida *et al.* (2005) [17] formed CH_4-CO_2 hydrates and found that when the gas phase consisted predominantly of CO_2, CH_4 preferentially forms hydrates in the early stages of hydrate formation. The observed data are consistent with these observations though merits further investigation to understand the implication in natural CH_4 hydrate reservoirs.

Figure 12. Time resolved visual observations of the CH_4-CO_2 hydrate phase at the end of formation and during dissociation for Run 5 at: (**a**) 460 psig, −1.05 °C; (**b**) 564 psig, 1.24 °C; (**c**) 635 psig, 2.44 °C; (**d**) 848 psig, 10.25 °C. These P/T conditions correspond to the numbers shown in the dissociation plot of Figure 11 where point 1 in Figure 11 represents (a) shown below.

(**a**)

(**b**)

(**c**)

(**d**)
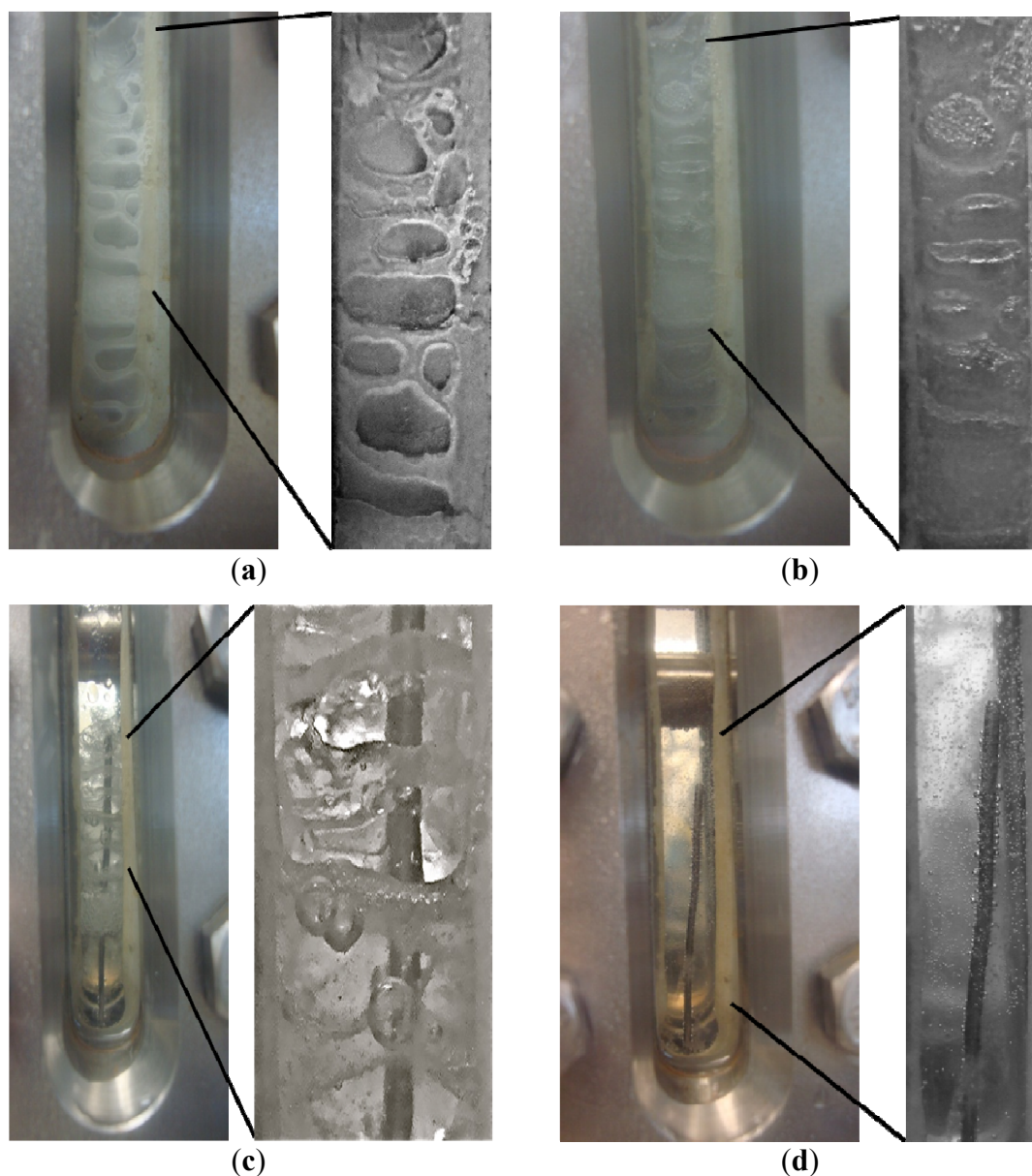
4. Conclusions

A facile formation of CO_2 hydrates was observed at high pressures and temperatures above freezing in a system in which water was in excess. The formed hydrates were found to accumulate in the aqueous phase at the bottom of the cell and not at the gas-liquid interface. The liquid interface was observed to be intact throughout the hydrate formation phenomenon which indicates that hydrates may have nucleated in the bulk solution or at the gas-liquid interface and then accumulated in the aqueous phase due to density difference.

The hydrate formation time was found to vary from 17 h to seven days. The conversion of about 32% of CO_2 gas into hydrates was measured when SDS, a known hydrate former, was present. The overall CO_2 hydrate yield could be increased with multiple gas charges though subsequent hydrate yield was low. This is explained by the decreased concentration of SDS in the solution as SDS tends to precipitate out after single use. A finding that CH_4-CO_2 gas mixtures that are CH_4-rich yield a higher concentration of CH_4 hydrates is contradictory to many previous findings, though these studies did not have gas mixtures made of predominantly CH_4. This system needs further study. CH_4 preference when forming gas hydrates from gas mixtures could be an important factor if CO_2 sequestration in the CH_4 free zone under the ocean floor is proposed. We are now investigating the use of computed tomography at the National Synchrotron Light Source (NSLS) to establish the morphology and stability of CO_2 hydrates formed from CH_4-CO_2 gas mixtures.

Acknowledgements

References

1. *2010 Carbon Sequestration Atlas of the United States and Canada*, 3rd ed.; National Energy Technology Library: Pittsburgh, PA, USA, 2010. Available online: http://www.netl.doe.gov/technologies/carbon_seq/refshelf/atlasIII/index.html (accessed on 26 June 2012).
2. Wang, Z.; Fu, Z.; Zhang, B.; Wang, G.; Rudolph, V.; Huo, L. Adsorption and desorption on coals for CO_2 sequestration. *Min. Sci. Technol. (China)* **2009**, *19*, 8–13.
3. Ravagnani, A.T.F.S.G.; Ligero, E.L.; Suslick, S.B. CO_2 sequestration through enhanced oil recovery in a mature oil field. *J. Petrol Sci. Eng.* **2009**, *65*, 129–138.
4. Rosenbauer, R.J.; Koksalan, T.; Palandri, J.L. Experimental investigation of CO_2-brine-rock interactions at elevated temperature and pressure: Implications for CO_2 sequestration in deep-saline aquifers. *Fuel Process Technol.* **2005**, *86*, 1581–1597.
5. Siriwardane, H.J.; Gondle, R.; Smith, D.H. Influence of shrinkage and swelling properties of coal on geological sequestration of carbon dioxide. In *Proceedings of the 2006 SPE Annual Technical Conference and Exhibition*, San Antonio, TX, USA, 24–27 September 2006.

6. Goel, N. *In situ* methane hydrate dissociation with carbon dioxide sequestration: Current knowledge and issues. *J. Petrol Sci. Eng.* **2006**, *51*, 169–184.

7. Tohidi, B.; Yang, J.H.; Salehabadi, M.; Anderson, R.; Chapoy, A. CO_2 hydrates could provide secondary safety factor in subsurface sequestration of CO_2. *Environ Sci Technol.* **2010**, *44*, 1509–1514.

8. Sloan, E.D.; Koh, C.A. *Clathrate Hydrates of Natural Gases*, 3rd ed.; CRC Press: Boca Raton, FL, USA, 2008.

9. Ohgaki, K.; Takano, K.; Moritoki, M. Exploitation of CH_4 Hydrates under the Nankai Trough in Combination with CO_2 Storage. *J. Chem. Eng. Jpn.* **1994**, *20*, 121–123.

10. Ota, M.; Morohashi, K.; Abe, Y.; Watanabe, M.; Smith, R.L.; Inomata, H. Replacement of CH_4 in the hydrate by use of liquid CO_2. *Energy Convers. Manag.* **2005**, *46*, 1680–1691.

11. Lee, H.; Seo, Y.; Seo, Y.T.; Moudrakovski, I.L.; Ripmeester, J.A. Recovering methane from solid methane hydrate with carbon dioxide. *Angew. Chem. Int. Ed.* **2003**, *42*, 5048–5051.

12. Sugaya, M.; Mori, Y.H. Behavior of clathrate hydrate formation at the boundary of liquid water and a fluorocarbon in liquid or vapor state. *Chem. Eng. Sci.* **1996**, *51*, 3505–3517.

13. Ripmeester, J.A.; Alavi, S. Molecular simulations of methane hydrate nucleation. *ChemPhysChem* **2010**, *11*, 978–980.

14. Lee, J.W.; Zhang, J.S.; Lee, S. Does SDS micellize under methane hydrate-forming conditions below the normal Krafft point? *J. Colloid Interf. Sci.* **2007**, *315*, 313–318.

15. Wu, Q.; Zhang, B. Memory effect on the pressure-temperature condition and induction time of gas hydrate nucleation. *J. Nat. Gas Chem.* **2010**, *19*, 446–451.

16. Seo, Y.T.; Lee, H.; Yoon, J.H. Hydrate phase equilibria of the carbon dioxide, methane, and water system. *J. Chem. Eng. Data* **2001**, *46*, 381–384.

17. Uchida, T.; Ikeda, I.Y.; Takeya, S.; Kamata, Y.; Ohmura, R.; Nagao, J.; Zatsepina, O.Y.; Buffett, B.A. Kinetics and stability of CH_4-CO_2 mixed gas hydrates during formation and long-term storage. *ChemPhysChem* **2005**, *6*, 646–654.